Contents lists available at ScienceDirect

# Journal of Sound and Vibration

journal homepage: www.elsevier.com/locate/jsvi

# The influence of energy recovery on the overall efficiency of acoustic sources at low frequencies

F. Tajdari [a,*], A.P. Berkhoff [a,b], R.A.R. van der Zee [c], A. de Boer [a]

[a] *University of Twente, Faculty of Engineering Technology, Drienerlolaan 5, 7500 AE Enschede, the Netherlands*
[b] *TNO Technical Sciences, Acoustics and Sonar, Oude Waalsdorperweg 63, 2597AK Den Haag, the Netherlands*
[c] *University of Twente, Faculty of Electrical Engineering, Drienerlolaan 5, 7500 AE Enschede, the Netherlands*

## ARTICLE INFO

## ABSTRACT

This paper defines a criterion called the overall efficiency (OE) for evaluating the efficiency of acoustic sources. In practice, the conventional efficiency (CE), is not capable of giving a comprehensive overview of the power consumption, especially in the connected amplifier drivers. The reason for this is that the CE is defined based on the nominal input electrical power. The nominal input electrical power is defined as the real part of the power that is delivered by the electrical amplifier to the actuation unit of an acoustic source. Therefore, power loss in the amplifier unit is not included in the CE definition. With the aid of the OE criterion, the effect of power loss in the connected amplifier units is taken into account. In particular, the application of the OE is crucial for acoustic sources that operate in a low frequency range. This is due to the reactive nature of power in both actuators and connected amplifiers. In the current paper, various combinations of amplifiers and actuators are studied. In particular, voice coil actuators and piezoelectric stack elements including both Lead Zirconate Titanate (PZT) ceramics and single crystal Lead Zirconate Niobate-Lead Titanate (PZN-PT) piezoelectric materials are investigated. In addition, the effect of a connected power driver is investigated. A class AB and a class D amplifier are studied respectively as analogue and switching amplifiers. Unlike a class AB amplifier, a class D amplifier is capable of energy recovery. A perforated flat acoustic source is examined in this paper as a practical example to verify the OE criterion. The numerical simulation on a thin acoustic source shows that for a single actuator, thanks to energy recovery, the OE is higher in a class D amplifier than in a class AB amplifier. This study reveals that if a class D amplifier is the driver, using piezoelectric actuators results in a higher OE compared to using a voice coil actuator. Measurements on the sample acoustic source verify the numerical results presented in the current study.

© 2020 Elsevier Ltd. All rights reserved.

## 1. Introduction

Thin acoustic sources can have advantages for active noise control [1], and for audio reproduction [2] in application with severe space constraints. Various combinations of loudspeaker drivers and structural radiation aids can be used in the acoustic source designs [3]. The loudspeaker driver is the actuation unit that converts electrical input power to a mechanical vibration, and the mechanical vibration generates sound [3]. Structural radiation aid units such as horns, baffles, or enclosures support

---

* Corresponding author.

*E-mail addresses:* f.tajdari@alumnus.utwente.nl (F. Tajdari), a.p.berkhoff@utwente.nl (A.P. Berkhoff), r.a.r.vanderzee@utwente.nl (R.A.R. van der Zee), a.deboer@utwente.nl (A. de Boer).

the quality of power conversion from the driver to the radiated sound [3]. Conventional moving coil loudspeakers are designed to produce an ideal rigid piston-like motion of moving panels. According to the ideal moving coil loudspeaker, all points on the panel vibrate in phase [3]. However, in practice, the frequency response of the moving coil loudspeakers is uneven due to unwanted bending mode shapes [3]. Distributed mode loudspeakers (DMLs) operate according to the concept of uniformly distributed, free bending wave vibration in a stiff, light panel [4]. Unlike the conventional piston-like moving coil loudspeakers, DMLs benefit from the random vibration of the points on the radiating panel to generate sound with uniform directivity [4–6]. Although DMLs are quite promising at high frequencies, they lead to complicated numerical computations and less accurate responses at low frequencies [4–6]. Electroactive polymers (EAPs) [7,8] act like piezoelectric materials. According to a review in Refs. [9], dielectric elastomer (DE) loudspeakers are lightweight structures made of EAPs with applications in acoustic transmission loss, sound reproduction systems, adaptive acoustic absorption for noise control, and sound generation. Heuss et al. [10] investigate the use of EAPs in a double-glazed window with an air cavity in between, to reduce sound transmission and sound radiation. They apply both semi-passive (by using Helmholtz resonators) and active (by using Electroactive Polymers as the acoustic actuators) treatments for acoustic transmission reduction. Although DEs are quite promising in sound transmission loss, they have a low coupling factor up to 0.3 that leads to a low efficiency of electro-mechanical coupling. Perforated panels have been studied in passive treatments for acoustic insulation and sound transmission [11–15], and for sound absorption [16–19], especially at low frequencies. In Ref. [20], active control techniques are used to reduce sound radiation from a honey-comb flat panel to control sound transmission. Although flat perforated panels are investigated in a few studies, there seem to be not so many currently used sandwich acoustic sources in practice. One available actively-controlled compact acoustic source that focuses on realizing a thin device at low frequencies is described by Berkhoff [21]. Berkhoff uses a sandwich panel in the structure of a thin acoustic source. Ho et al. [22,23] investigate techniques to control the vibration of the suggested honey-comb structure in Ref. [21] as a compact acoustic source. Ho et al. use five uniformly distributed voice coil actuators. This model has some advantages compared to other acoustic sources. For instance, the authors apply active control techniques to the honey-comb plate to damp the bending mode shapes of the acoustic source.

In most acoustic source systems, the conventional efficiency (CE) parameter is acceptably used as a common criterion to compare acoustic sources [3]. The CE is an expression that relates the output radiated power to the required electrical power of the loudspeaker systems [3]. The effect of connected source driver, i.e. the connected amplifier, is neglected in this definition [3]. However, in practice, a large amount of input electrical power to acoustic source drivers is dissipated in the power supply unit. This inevitable power dissipation occurs in both connected amplifier driver and actuator units, especially at low frequencies. Due to power loss in the driver unit, a major part of the supplied electrical power is lost before being delivered to the acoustic source. In the current paper, a criterion for acoustic sources is introduced: the overall efficiency (OE). This criterion is applicable to all loudspeaker systems. The OE takes the power dissipation in the connected driver unit into account in addition to the power loss in the actuators. Therefore, it can give a fair comparison for a wide range of driver-source combinations of acoustic sources.

Voice coil actuators are the most common ones among the acoustic source systems [3]. However, due to electrical resistance of voice coil actuators, a major part of the supplied power is lost before being delivered to moving coil loudspeakers. Moreover, at low frequencies, a major part of the delivered power to acoustic sources is stored in the reactive components. As a result of power dissipation and storage in both the power supply unit and the acoustic source, a small amount of active power is delivered to the radiating part of the acoustic source. Therefore, the existence of an energy recovery unit is crucial in order to decrease the demand for extra electrical input power. On the other hand, in the case an appropriate amplifier is used, the recovered power from the acoustic source has to pass along the resistors of voice coil actuators again. As a result, the recovered power is dissipated again in the actuator unit, and eventually, not so much power can be reused. Therefore, the power supply unit has to be modified in such a way that the connected amplifier not only is compatible with the actuators, but is able to recover the stored power by operating in the inverse direction.

To increase the OE of acoustic sources that operate at low frequencies, one possibility is to use piezoelectric actuators as the excitation units. The reason is that these actuators do not have large dissipation compared to voice coil actuators, in particular in quasi-static conditions. At low frequencies, piezoelectric elements are mainly electrical capacitive loads. Therefore, a wide range of studies have been dedicated to investigating the proper power amplifiers to drive these actuators. For example, some studies [24,25] have investigated bidirectional class B amplifiers as the power driver for the piezoelectric stack actuators. As a result, they achieve up to 50% improvement in the efficiency of the actuators by combining a class B amplifier with a switching circuit. In addition, amplifiers with current control techniques have been used to drive a piezoelectric element. For instance, in Ref. [26], a suggested high-voltage amplifier leads to a ripple-free actuation while using a current feedback control unit. The authors in Ref. [27], use an equivalent electrical circuit to model piezoelectric actuators. With the use of a feedback control technique, up to 80% of the input power is recovered. In Refs. [28], designing a power driver capable of charge recovery results in generating a quasi-square signal as an input for the actuators. Chao et al. [29] suggest a power driver circuit to drive a low-voltage piezoelectric actuator in a micro-pump device using a differential amplifier. A variety of studies address the switching techniques to drive the piezoelectric actuators by varying the number of switches in the circuit configuration [30–34]. Furthermore, Edamana et al. [35] suggest an optimum circuit to drive a piezoelectric actuator in a precise positioning application. By applying control techniques, they succeed to optimize the amount of charge recovery while using the maximum voltage across the piezoelectric element in the simulation. A power amplifier is designed in a research performed by Stiebel and Janocha [36–38]. They suggest a time detection technique to control the performance of the switches. Moreover, they introduce a so called "hybrid amplifier" to optimize the power recovery. Their suggested circuit combines the high efficiency of a class D amplifier with the high signal quality of a class AB amplifier. The result shows that the suggested model converts the input DC signal into an AC signal. In

addition, using their circuit, which is based on an intelligent switching technique, the amount of recovered power is optimized.

Equivalent electrical circuits are simple solutions to modeling complicated systems. For instance, in Ref. [39] various lumped models of the piezoelectric elements are represented as equivalent electrical circuits. A lumped model of a synthetic jet actuator is investigated in Ref. [40] to include the electroacoustical parts such as cavity. In Refs. [41], an electromechanical Helmholtz resonator is designed using an equivalent lumped model. Prasad et al. [42] use a two-port lumped electrical network to analytically model a piezoelectric composite transducer. A comprehensive review on the available studies is addressed in Ref. [43] to investigate energy harvesting from a cavity using the electrical circuits.

Here, we investigate the possible options to increase the OE of acoustic sources operating at low frequencies. In this research, the frequencies between 20 Hz and 1000 Hz are assumed as low frequencies. The focus of this study is to find the most efficient amplifier-actuator combination for acoustic sources in a low frequency range. In particular, the most commonly used actuators, i.e. voice coil actuators, and the capacitive piezoelectric stack actuators are studied in the current research. The thin acoustic source designed by Ho et al. [22] is investigated to verify the proposed OE criterion using the amplifier-actuator configurations. A lumped model of the suggested acoustic source is used to investigate the performance of the compact lumped system. To improve the power supply unit, two major classes of amplifiers are investigated with the focus on the energy recovery possibilities. In addition, to improve the OE of the lumped acoustic source, the performance of both voice coil and piezoelectric stack actuators are numerically and experimentally investigated.

The contribution of the current study is to propose another efficiency criterion applicable to all acoustic source systems with any amplifier-actuator configuration. The OE for general acoustic source is investigated in Part I of this paper. To verify the proposed criterion, a thin perforated acoustic source is examined in Part II. An equivalent electrical circuit of a piezoelectric actuator is combined with a lumped model of the thin acoustic source. Using the OE criterion, it is concluded that the combination of a class D amplifier and an appropriate actuator leads to recovering the stored power in the thin acoustic source system. This energy recovery leads to maximizing the OE of such a flat sandwich acoustic source, especially for frequencies between 20 Hz and 1000 Hz.

## 2. Part I: general approach: a generic acoustic source

### 2.1. Energy and power

Power is defined as the rate of producing or consuming energy by a system [44]. In an acoustic source system connected to the electrical actuator and amplifier units, the power in a component is the rate of energy conversion, storage and consumption. The term power is used in this paper to quantify, measure and compare the input and output energy rates in various components of an acoustic source system. In this paper, the power for sinusoidal signals is used to quantify or measure the two efficiency criteria.

### 2.2. Definition of efficiency

Conventional efficiency is commonly used to compare loudspeaker systems [3]. It is defined as the ratio of the acoustic source output power to the actuators' nominal input electrical power [3]. The nominal input electric power in the CE definition is the power that is delivered by the electrical amplifier into a resistor having the same value as the driver voice coil resistance (see Refs. [3] for more details). As seen in Fig. 1, the CE is expressed as:

$$\eta_{CE} = \frac{P_{rad}}{P_{in,act}}. \tag{1}$$

where $P_{in,act}$ and $P_{rad}$ are frequency dependent time-averaged powers for time-harmonic input and output powers. The effect of the connected electrical amplifier driver is neglected in Eq. (1). In practice, the delivered power to the actuation unit, $P_{in,act}$, is a fraction of the total electrical power that is supplied to the amplifier ($P_{in,amp}$ in Fig. 1). At low frequencies (between 20 Hz and 1000 Hz), a limited active power is available to the acoustic sources. The reason is that a major portion of the supplied power is stored in reactive elements of the acoustic sources [45]. If an appropriate amplifier unit is present, the stored reactive power has the capability of being reused. Using the OE criterion, the capability of an acoustic source system to reuse the stored reactive power is examined. The OE is defined as:

$$\eta_{OE} = \frac{P_{rad}}{P_{in,amp}}. \tag{2}$$

Using the definition of the OE in Eq. (2), the power loss in an amplifier unit can be identified. As an estimation, the OE and CE are related using the following equation:

$$OE = CE \times \eta_{amp} \tag{3}$$

where $\eta_{amp}$ is the efficiency of the connected amplifier. The amplifier efficiency is a function of the operating frequency and is dependent on the nature of the connected acoustic source as a load. In addition to the operating frequency, the active and reactive portions of the acoustic source components have influence on $\eta_{amp}$. According to Eq. (3), the effect of the connected
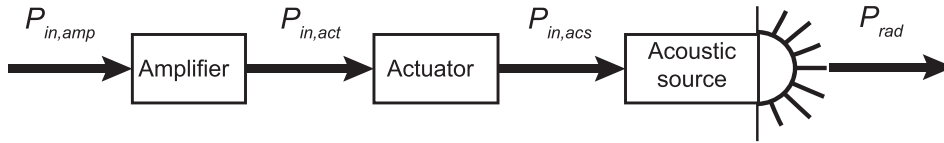
**Fig. 1.** Power input-output scheme that is used for efficiency definition.
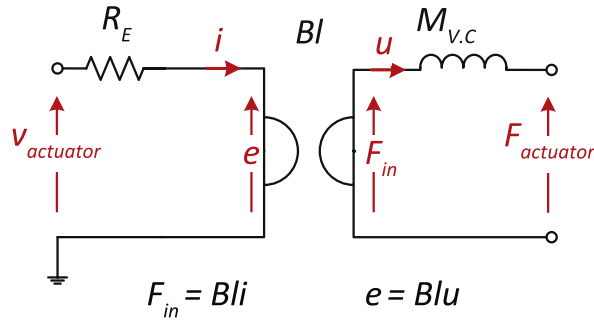


**Fig. 2.** Equivalent electrical circuit of a voice coil actuator.

amplifier is taken into account in the OE. A proper combination of amplifiers and actuators can lead to the highest OE for any acoustic source. Using the OE criterion, the most common actuators and amplifiers are investigated in details in the following, to find the most efficient combination. In addition, the effect of an appropriate combination of amplifiers and actuators on the OE of a general acoustic source that operates at low frequencies is discussed in Section 2.5.

### 2.3. Actuators

An actuator provides the driving force for the acoustic source. One of the most commonly used actuators in loudspeaker systems is the voice coil actuator. Voice coil actuators have a resistive nature. Another actuator type that is studied in this paper is a piezoelectric actuator. Piezoelectric actuators have capacitive nature, especially at low frequencies. Due to their capacitive nature, piezoelectric devices can be interesting when they are connected to appropriate amplifiers.

#### 2.3.1. Voice coil actuators

One can find the equivalent electrical circuit of a voice coil actuator in both Fig. 2 and Table 1, where $Bl$, $M_{V.C}$ and $R_E$ show the voice coil electromechnical conversion coefficient, mass and electrical resistance, respectively.

According to this figure, the only resistive element in the equivalent electrical circuit of a voice coil actuator is the electrical resistor, $R_E$. $R_E$ dissipates the majority of the electrical input power in the actuator unit.

#### 2.3.2. Piezoelectric actuators

The equivalent electrical circuit of a piezoelectric stack actuator is shown in Fig. 3. Electrical elements $M_p$, $C_p$ and $R_p$, in the equivalent electrical circuit represent the mass, mechanical compliance and mechanical damping of the piezoelectric actuator, respectively. $\alpha$ is the electromechanical conversion coefficient, and $C_0$ shows the electrical capacitive load of the piezoelectric device. The negative capacitor shows a coupling between the electrical and mechanical domains and has the same value of $C_0$. One can distinguish the electrical ($C_0$) and mechanical ($C_p$) capacitors. $C_0$ stores the main portion of the input electrical power during the charge cycle, while $C_p$ shows the spring nature of a piezoelectric device from mechanical point of view. The electrical

**Table 1**
Parameters of the equivalent electrical circuit of piezoelectric and voice coil actuators.

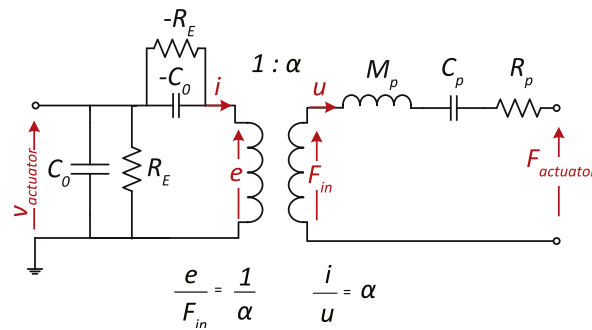| Parameter | Symbol | SI Unit |
|---|---|---|
| Input current in the electrical domain | $i$ | A |
| Velocity | $u$ | ms$^{-1}$ |
| Input voltage to actuator | $v_{actuator}$ | V |
| Output voltage in the electrical domain | $e$ | V |
| Input force to the mechanical domain | $F_{in}$ | N |
| Output force of the actuator | $F_{actuator}$ | N |

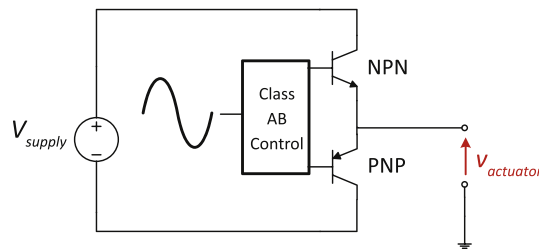**Fig. 3.** Equivalent electrical circuit of a piezoelectric stack actuator.



**Fig. 4.** Electrical circuit of a class AB amplifier.

power dissipation in the electrical resistor $R_E$ is small compared to the same power dissipation in the voice coil actuator. The coupling factor of the piezoelectric actuator shows the amount of electrical input power that is not stored in the electrical capacitor, but is transferred to the mechanical domain. The description of the electrical circuit of a piezoelectric stack actuator is listed in Table 1. For more details the reader is referred to Ref. [45].

Both the dissipated power in the voice coil actuator and the capacitive power stored in the piezoelectric actuator lower the actual power that is transferred from the actuator unit to the acoustic source. As a result, the existence of an appropriate amplifier capable of recovering the stored power is crucial to increase the transferred power to the acoustic source while decreasing the required total electrical input power.

## 2.4. Amplifiers

The power driver unit supplies the electrical power to the actuators. In this study, two different classes of power amplifiers are investigated; class AB and class D amplifiers. The latter is capable of energy recovery and can be interesting when it is combined with various actuators.

### 2.4.1. Class AB amplifiers

A class AB power driver is shown in Fig. 4. This amplifier has a high quality output signal, and is interesting for precise positioning applications when a feedback loop is added. Therefore, when the energy cost is not the first priority, but the quality is, a class AB amplifier is an appropriate option. However, a class AB amplifier is unable to recover the stored energy in the actuator during the discharge cycle. Therefore, all the stored energy is dissipated eventually. In addition, since the output transistors have a voltage drop across them when delivering current, they also dissipate when delivering power to the load. This power dissipation causes a class AB amplifier to be inefficient and costly in general applications, where the efficiency is a significant design factor.

### 2.4.2. Class D amplifiers

A class D amplifier, on the other hand, is more energy efficient compared to a class AB amplifier. The schematic of a class D amplifier is shown in Fig. 5. As seen in the figure, switches $SW_1$ and $SW_2$, and a comparator lead to generation of a Pulse-Width Modulation (PWM) signal, and $V_{supply}$ is a DC voltage source. The details of a class D amplifier are described in Ref. [38]. A class D amplifier is able to recover the reactive power stored in both the acoustic source and the actuator during discharge [38]. Since it is a switching amplifier, the dissipated power in the driver unit is very small compared to that in a class AB amplifier. A low-pass filter is used in the output port of a class D amplifier to filter out the switching frequency and harmonics that have very high energy. However, the output signal is not always of high quality. This is due to the difficulties of applying feedback in the presence of a second order low-pass filter in the loop.
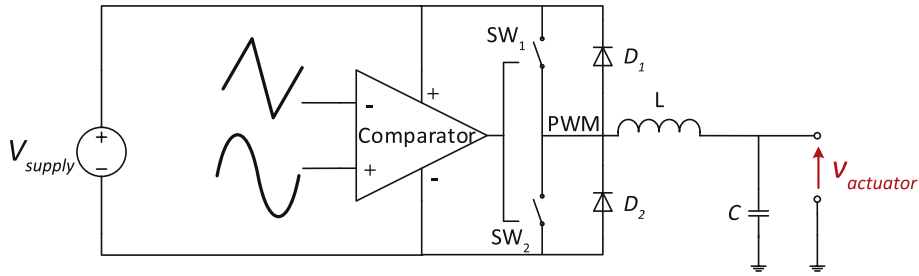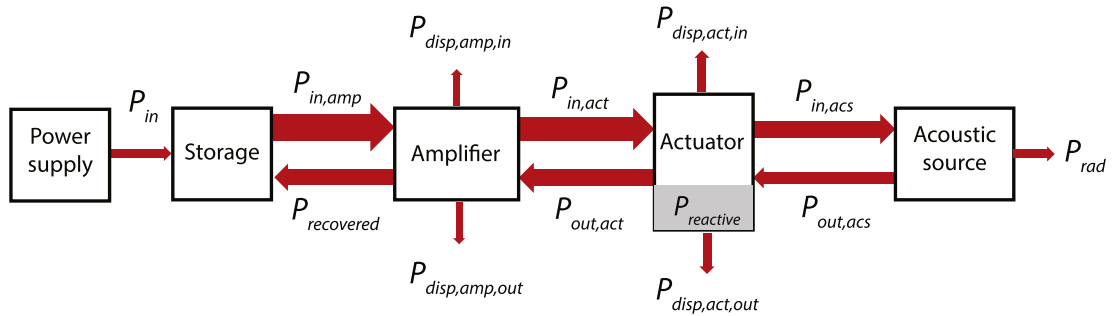
**Fig. 5.** Electrical circuit of a class D amplifier.



**Fig. 6.** Power flow in an arbitrary acoustic source operating at low frequencies.

### 2.5. Overall efficiency for a general acoustic source

At low frequencies, acoustic sources are expected to have a low OE. This is mainly due to low radiation efficiency of the acoustic sources at low frequencies when the size of the source is much smaller than a wavelength. Moreover, depending on the reactive nature of the connected actuators and the acoustic source components, some portions of the input supplied power can remain unused while some portions are dissipated. The unused portion of the input power is not dissipated but stored, and can be recovered completely when it is electrical and partly when it is mechanical. The unused power can only be recovered and reused with the aid of an appropriate electrical amplifier. The influence of the connected amplifier on recovering the stored reactive power in an arbitrary acoustic source system and the resulting OE are investigated in this section.

Fig. 6 shows the power flow in an arbitrary acoustic source that operates at low frequencies. According to Eq. (2), the OE is defined as the ratio between the output acoustical radiated power of the acoustic source, $P_{rad}$, to the input supplied power from the power supply unit, $P_{in}$. If the amplifier is capable of recovering the unused power, then $P_{in} = P_{in,amp} - P_{recovered}$. For amplifiers capable of power recovery, for instance class D amplifiers, a smaller $P_{in}$ is required for the acoustic source system. Therefore, acoustic sources connected to class D amplifiers have higher OE than sources connected to class AB amplifiers.

As seen in Fig. 6, the connected actuation unit also has an influence on the OE and the recovered power. If an actuator, for instance a voice coil actuator, dissipates a large portion of the input power as $P_{disp,act,in}$, the available power for the acoustic source ($P_{in,acs}$) is limited. In addition, a large portion of the recovered power is dissipated in the actuation unit as $P_{disp,act,out}$. Due to an insignificant recovered power in a voice coil actuator, a large $P_{in}$ is needed. This large $P_{in}$ results in a low OE for a voice coil actuator that is connected to an amplifier capable of power recovery. On the other hand, if an actuator with small power dissipation is used, higher recovered power is available to the connected amplifier. Therefore, the resulting OE can be higher. The OE in this case is dependent on the reactive nature of the connected actuator. For example, if a piezoelectric actuator is used, a large portion of the input power is stored in the actuation unit as $P_{reactive}$. This unused power is a function of the operating frequency, the reactive portion of the actuator impedance and the phase shift between the current and voltage to the actuator. Therefore, the obtained OE is also dependent on the operating frequency, the actuator reactive nature and the phase shift. According to Fig. 6, a correct combination of the amplifier and actuator can lead to a high OE of the acoustic source that operates at low frequencies. The figure shows the influence of recovered power on the OE of an arbitrary acoustic source. The choice of the actuator also depends on other factors such as maximum displacement capability and harmonic distortion, which are beyond the scope of this paper.

### 2.6. A general analytical approach for an acoustic source

An analytical study in Figs. 7 and 8 reveals the amount of power flow in an arbitrary acoustic source [45]. In this study, it is assumed that the acoustic source is operating at the fundamental resonance frequency [45]. The reason is that the maximum power flow in the acoustic source occurs at the resonance. The resonance frequency allows for common efficiency values of
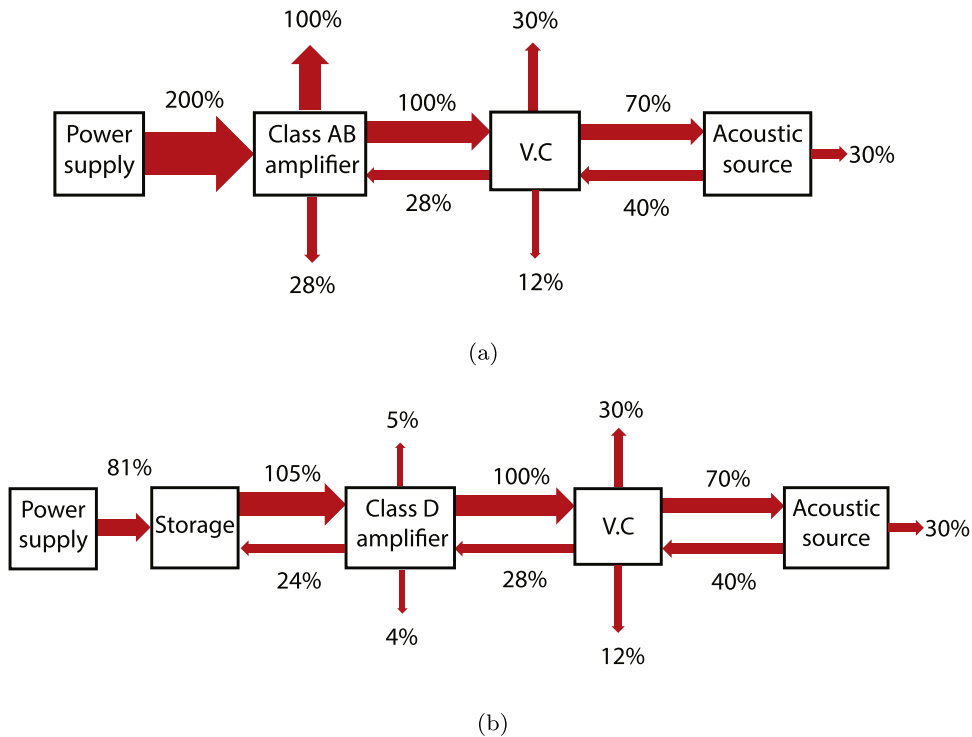
Fig. 7. The power flow through an arbitrary acoustic source that is actuated by a voice coil actuator. The values in the figure are scaled with respect to the input power to the actuator as the reference (100%): (a) class AB amplifier; (b) class D amplifier.

the connected actuators and amplifiers. Combinations of the two actuators (voice coil and piezoelectric actuators) and the two amplifiers (class AB and class D amplifiers) are considered. In this analytical analysis, the input power to the actuation unit of the acoustic source is considered as the reference level (100%). Therefore, other power flows are scaled with respect to this reference power. The acoustical power radiation of the arbitrary acoustic source, $P_{rad}$ can be chosen independently to obtain the OE in this section. In the remainder of this section, it is assumed that $P_{rad} = 30\%$. This value can be corrected when a specific acoustic source is used in practice.

Fig. 7 shows the power flow in an acoustic source with the voice coil actuator. At resonance, the voice coil actuator dissipates approximately 30% of the input power. In the case of a class D amplifier, 24% of the power demand can be recovered. Therefore, $P_{in} = 81\%$ extra input power is needed from the power supply unit (see also Fig. 6). On the other hand, a class AB amplifier cannot recover the unused power and dissipates it eventually. As a result, the power supply unit has to provide twice the reference power to the connected amplifier. As seen in Fig. 7, the OE for a voice coil actuator connected to both class AB and class D amplifiers is respectively $30/200 \times 100 = 15\%$ and $30/81 \times 100 = 37\%$.

The combination of the two amplifiers and the piezoelectric actuator is shown in Fig. 8. When a class D amplifier is used, $P_{in} = 39\%$ of the reference power is required from the power supply unit (see also Fig. 6). Furthermore, approximately 66% of the power demand can be recovered and reused. A class AB amplifier, however, has to deliver twice the reference power. As a result, $(200 - 39)/200 \times 100 = 80.5\%$ of the input electrical power is saved when using a class D amplifier instead of a class AB amplifier. Therefore, for a piezoelectric actuator, the OE of the acoustic source can reach $30/200 \times 100 = 15\%$ and $30/39 \times 100 = 76\%$ at resonance respectively for a class AB and a class D amplifier.

The analytical approach shows that using a class D amplifier connected to a piezoelectric actuator improves the performance of any arbitrary acoustic source operating at low frequencies in terms of the required input electrical power and the resulting OE. It has to be noted that the analytical approach in this section is an estimation of the common OE of an acoustic source when it operates at the resonance. In practice, the efficiency of the connected amplifier and actuator is dependent on the operating frequency, the phase shift between the supplied current and voltage and the reactive nature of the acoustic source system, which the latter is also a function of the operating frequency. As a result, further investigation is needed for an acoustic source to determine the OE, especially at low frequencies. To verify the dependency of the OE on the operating frequency and the nature of the acoustic source load, in the remainder of this paper, a small sample of a thin acoustic source is investigated.

## 3. Part II: case study: a flat acoustic source

The flat acoustic source introduced in Refs. [22,45] is used as a case study. The combination of the flat acoustic source with various amplifiers and actuators, which have been introduced in Part I, is investigated. Four resulting combinations of the two
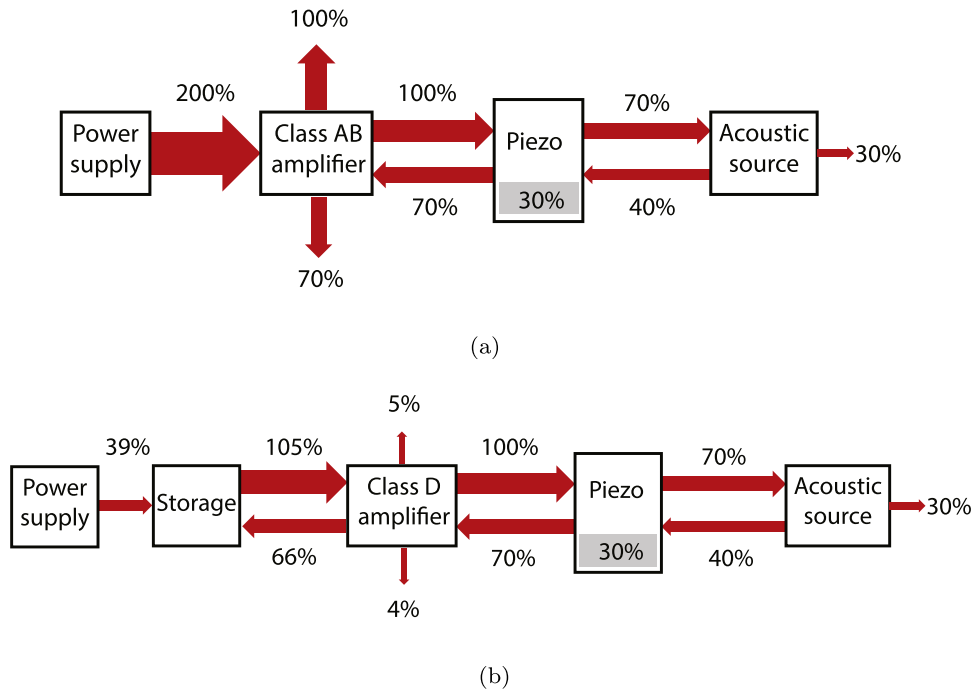
(a)



(b)

**Fig. 8.** The power flow through an arbitrary acoustic source that is actuated by a piezoelectric actuator. The values in the figure are scaled with respect to the input power to the actuator as the reference (100%) [45]: (a) class AB amplifier; (b) class D amplifier.
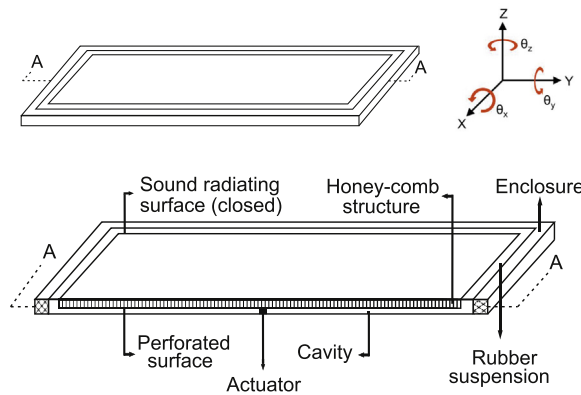


**Fig. 9.** The thin acoustic source with A–A cross section view that is studied in this paper [45].

actuators (voice coil and piezoelectric actuators) and the two amplifiers (class AB and class D amplifiers) are considered. The OE of the flat acoustic source is studied numerically and experimentally to determine the effect of power recovery. The result of this case study reveals the dependency of the OE on the operating frequency, the capability of the connected amplifier in power recovery and the reactive nature of the connected actuator.

### 3.1. The flat acoustic source

The schematic of the sample flat acoustic source, which is studied by Ho et al. [22], is shown in Fig. 9. It consists of a thin radiating surface with a thickness of 0.125 mm. At low frequencies (between 20 Hz and 1000 Hz), the efficiency of an acoustic source is proportional to the enclosure volume [3]. Because of the small dimension in the direction of the $z$-axis, the surface area of the source has to be relatively large in order to get a reasonable efficiency [21]. The surface area of the thin acoustic source in this study is the same size as a standard $A_4$ paper, i.e. 297 mm $\times$ 210 mm. The upper vibrating surface is attached to the top surface of a honey-comb structure, so that the resulted sandwich panel has higher bending stiffness compared to a single thin panel. The lower surface of the honey-comb structure is perforated and is in interaction with the air inside an air cavity
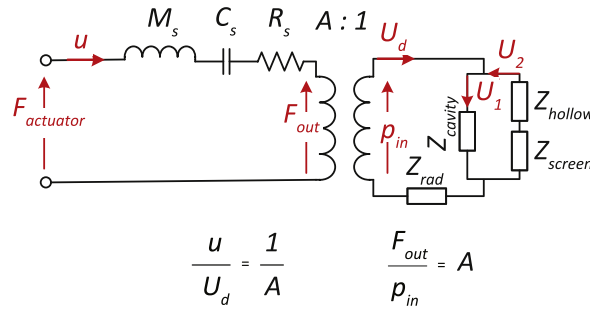
**Fig. 10.** Equivalent electrical circuit of the lumped acoustic source.

(see Fig. 9). During the operation of the acoustic source, the air inside the cavity is compressed and expanded while entering and leaving the hollows of the honey-comb structure through the holes of the perforated plate. In the actuation unit, the driving force of the actuators moves the acoustic source in the out-of-plane direction (in the direction of the z-axis). The suggested sandwich panel has a thickness of approximately 22 mm in the direction of the z-axis, while it is stiff enough to reduce the modal complexity of the active control analysis [21]. The perforated panel combines the low density with the high bending stiffness. The low density and the high stiffness lead to a fundamental resonance at high frequencies. Therefore, a uniform displacement of the suggested flat acoustic source is ensured in a wide range of frequencies in this research [21].

Although the frequency response of the suggested acoustic source by Ho et al. [22] is relatively flat, a large amount of the input power to the sandwich acoustic source is dissipated in the power supply unit. The power dissipation occurs in the connected voice coil actuators and the amplifier driver, especially at low frequencies.

In this study, a lumped model of the thin acoustic source is developed. The lumped model is connected to the actuator-amplifier combinations that are introduced earlier in this paper. The OE of various combinations of the two actuators, the flat acoustic source and the two amplifiers is numerically evaluated. Experimental results are used for verification of the numerical analysis.

### 3.2. Lumped model of the flat acoustic source

A lumped model of the thin acoustic source is considered in this study. This assumption is valid in the frequency range in which the wave length of the radiated sound is large enough compared to the largest dimension of the acoustic source [40]. In the current acoustic source, the largest dimension is in the direction of the y-axis (297 mm). This assumption holds for the frequency range of interest in this study. The reason is that the largest dimension of the acoustic source is smaller than the wave length for frequencies between 20 Hz and 1000 Hz.

Radiation impedance of the rectangular lumped acoustic source is modeled as the radiation impedance for a rigid circular piston. In this research, due to the complexity of the functions used in the Helmholtz integral [46], such as Bessel and Hankel functions, an approximation method is used to evaluate the radiation impedance of a circular piston. This approximation is valid for spherical sources [47]. The equivalent radius of the circular piston, $a$[m], is obtained considering the same surface area for both the equivalent circle and the primary rectangle. This equivalent circular piston vibrates in an infinite rigid baffle and radiates into half space. According to Ref. [47], a correction coefficient of 0.7 is used to convert the radius of a pulsating sphere ($a'$) into the radius of an equivalent baffled pulsating piston. Therefore, at low frequencies (from 20 Hz to 1000 Hz), the radiation impedance of a baffled pulsating piston in half space is defined by the following two equations assuming $a' = 0.7a$:

$$\frac{1}{Z_{rad}} = \frac{1}{R_{rad}} + \frac{1}{j\omega M_{rad}}, \tag{4}$$

$$R_{rad} = \frac{\rho_{air}c}{4\pi a'^2},$$

$$M_{rad} = \frac{\rho_{air}}{4\pi a'}, \tag{5}$$

where $\rho_{air}$[kgm$^{-3}$] and $c$[ms$^{-1}$] represent the density and speed of sound in air, respectively, and $\omega$[rads$^{-1}$] is the angular frequency. The total radiation impedance ($Z_{rad}$) is modeled as a resistor ($R_{rad}$) in parallel with an inductor ($M_{rad}$) from the electrical point of view.

The equivalent electrical circuit of the complete lumped acoustic source is shown in Fig. 10. Various parts of the acoustic source are simplified as their equivalent electrical elements, and are attached to the electrical circuit of the actuator. The mechanical mass, compliance and damping of the suspensions of the flat acoustic source are represented by $M_s$, $C_s$ and $R_s$, respectively. The parameters in Fig. 10 are introduced in Tables 1 and 2.

**Table 2**
Parameters of the equivalent electrical circuit of the thin acoustic source used in this research.

| Parameter | Symbol | SI Unit |
|---|---|---|
| Output force of the mechanical domain | $F_{out}$ | N |
| Input pressure of the acoustical domain | $p_{in}$ | Pa |
| Volume velocity | $U_d$ | $m^3 s^{-1}$ |
| Volume velocity trough the air cavity | $U_1$ | $m^3 s^{-1}$ |
| Volume velocity trough the hollows and the perforated plate | $U_2$ | $m^3 s^{-1}$ |

**Table 3**
Parameters of the equivalent electrical circuit of the lumped acoustic source [22].

| Parameter | Symbol | SI Unit | Value |
|---|---|---|---|
| Speed of sound in air | $c$ | $ms^{-1}$ | 343 |
| Density of air | $\rho_{air}$ | $kgm^{-3}$ | 1.21 |
| Dimensionless area porosity | $\sigma$ | – | 0.5 |
| Dynamic viscosity | $\mu$ | $kgm^{-1} s^{-1}$ | $1.864 \times 10^{-5}$ |
| Wave number | k | $radm^{-1}$ | $\frac{\omega}{c}$ |
| Plate thickness | $t_p$ | m | $1 \times 10^{-3}$ |
| Distance between the holes | $d_h$ | m | $5 \times 10^{-3}$ |

The acoustical impedances of the air in the lumped circuit are as follows:

$$Z_{cavity} = \frac{v_{cavity}}{\rho_{air}c^2},$$ (6)

$$Z_{hollows} = \frac{v_{h.c}}{\rho_{air}c^2},$$ (7)

in which the parameters $v_{cavity}$ and $v_{h.c}$ are the volume of air in the cavity and in the hollows of the honeycomb structure in [$m^3$], respectively. The acoustical impedance of the perforated panel is stated as:

$$Z_{screen} = \frac{\rho_{air}c\zeta_{screen}}{A},$$ (8)

where $A[m^2]$ is the surface area of the perforated panel and $\zeta_{screen}$ is formulated as follows:

$$\zeta_{screen} = \frac{2}{\sigma}\sqrt{\frac{2\mu k}{\rho_{air}c}}\left(\frac{t_p}{d_h} + 1 - \sigma\right) + j\frac{k}{\sigma}\left(t_p + 0.85d_h(1 - \sqrt{\frac{\sigma}{\pi}})\right).$$ (9)

According to Eq. (9), $\zeta_{screen}$ is a function of the dimensions of the holes in the perforated panel and the distance between two neighboring holes. The reader is referred to Refs. [48] for more details on derivation of Eq. (9). Parameters of this equation are defined in detail in Tables 1–3.

### 3.3. Numerical analysis

The properties of the thin acoustic source are shown in Table 4.

To have a fair comparison, in the numerical model, the mass of both voice coil and piezoelectric stack actuators is identical. The voice coil actuator used in this study is of type LA18-12-000A manufactured by BEI Kimco Magnetics [49], and its material properties are given in Table 5.

#### 3.3.1. Optimization

MATLAB R2015b optimization toolbox [50] is used to select the appropriate stack piezoelectric actuator in the structure of the $A_4$-sized thin acoustic source. As a result, the optimum dimensions (radius and length) of the cylindrical piezoelectric stack

**Table 4**
Properties of the $A_4$-sized honey-comb acoustic source.

| Parameter | Symbol | SI Unit | Value |
|---|---|---|---|
| Thickness | $l_z$ | mm | 22 |
| Density | $\rho_{h.c}$ | $kgm^{-3}$ | 201 |
| Compliance of the suspensions | $C_s$ | $mN^{-1}$ | $1.2 \times 10^{-3}$ |
| Mechanical loss | $R_s$ | $Nsm^{-1}$ | 7.45 |

**Table 5**
Properties of the voice coil actuator [49].

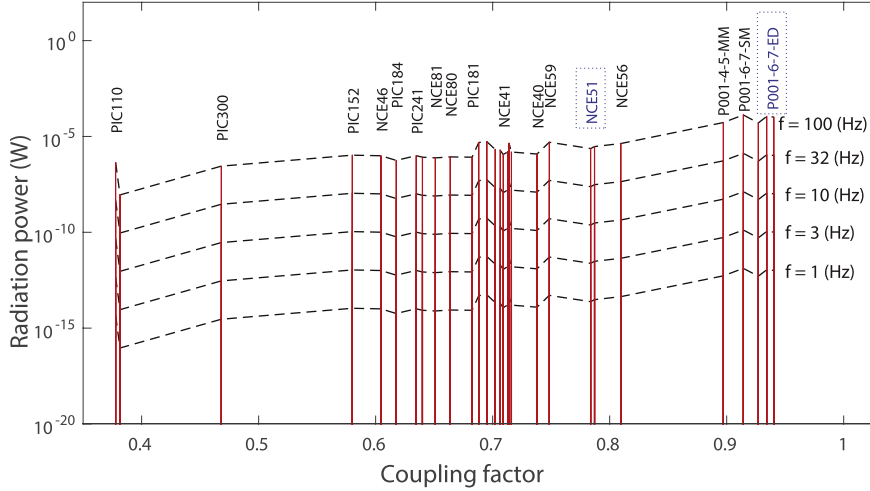| Parameter | Symbol | SI Unit | Value |
|---|---|---|---|
| Electromechnical conversion coefficient | $Bl$ | Tm | 13.2 |
| DC resistance of the coil | $Re$ | Ω | 8.85 |
| Mass | $M_{V.C}$ | g | 43.7 |



**Fig. 11.** The radiated power of the lumped acoustic source obtained for 29 different piezoelectric materials. The bar graph is sorted based on the materials' coupling factors. Materials NCE51 and P001-6-7-ED are chosen for evaluation in the numerical simulation as PZT and PZN-PT materials, respectively.

actuator for various already available piezoelectric materials are obtained. The following optimization problem is defined:

$$\underset{f,r_p,l_p}{\text{maximize}} \quad P_{rad}(f, r_p, l_p),$$

$$\text{subject to} \quad M_p = M_{V.C}, \tag{10}$$

where $f$ is the operating frequency in [Hz], and $r_p$ and $l_p$ are the radius and length of the piezoelectric stack actuator, respectively. According to Eq. (10), the only constraint is the mass of the piezoelectric stack actuator, $M_p$, that has to be equal to the mass of the voice coil actuator, $M_{V.C}$, to ensure a fair comparison. The objective is maximizing the radiation power ($P_{rad}$) of the acoustic source when it is excited by a piezoelectric stack actuator. The radiation power in Eq. (10) is instantaneous power and is defined using the electrical analogy shown in Fig. 10 as follows:

$$P_{rad} = R_{rad} U_d^2, \tag{11}$$

where $R_{rad}$ is obtained using Eq. (5) and $U_d$ is defined in Table 2. As seen in Fig. 10, $U_d$, which is the current along the acoustical elements, is a function of the force applied by the piezoelectric element. This applied force is directly related to the properties of the piezoelectric actuator, particularly, to the dimensions of the piezoelectric device.

The optimization result is shown in Fig. 11. This figure shows the radiation power of the lumped acoustic source at different frequencies. Twenty nine different piezoelectric stack actuators with various types of material are used in the performed optimization. Materials are shown in the bar graph in Fig. 11 and are sorted according to their coupling factors. Some of the materials' names are written in Fig. 11. As seen in the figure, the higher the coupling factor of the piezoelectric material, the higher the radiated power of the lumped acoustic source. Values of coupling factor above 0.9 in this figure, belong to single crystal piezoelectric materials.

Based on Fig. 11, one single crystal PZN-PT material with a coupling factor of 0.95 (MICROFINE Materials Technologies PTE LTD type: P001-6-7-ED) [51], and one ceramic PZT material with a coupling factor of 0.78 (Noliac type: NAC2013-HXX with material NCE51) [52] are chosen to be studied in detail in the remainder of this paper. The obtained optimized dimensions of these two piezoelectric stack actuators are $l_p = 73.3$ mm and $r_p = 4.87$ mm for PZT material, and $l_p = 71.1$ mm and $r_p = 4.81$ mm for single crystal PZN-PT material. The material properties of both PZT and PZN-PT piezoelectric elements are shown in Table 6.

*3.3.2. LTspice IV analysis*

After determining the optimum dimensions of the piezoelectric elements, the OE of the lumped acoustic source, $\eta_{OE}$, is investigated considering the effect of connected amplifiers. The OE gives the amount of radiated power, $P_{rad}$, of the lumped

**Table 6**
Material properties of piezoelectric actuators.

| Parameters | Symbol | Value | | SI unit |
|---|---|---|---|---|
| | | PZT [52] | PZN-PT [51] | |
| Material | – | NCE51 | P001-6-7-ED | – |
| Charge coefficient | $d_{33}$ | 443 | 2000 | $10^{-12}$ C N$^{-1}$ |
| Relative permittivity | $\frac{\epsilon^T}{\epsilon_0}$ | 1900 | 5200 | – |
| Elastic compliance | $s^E$ | 19 | 108 | $10^{-12}$ m$^2$ N$^{-1}$ |
| Density | $\rho_{piezo}$ | 7850 | 8350 | kgm$^{-3}$ |
| Dielectric loss factor | $\tan\delta$ | $150 \times 10^{-4}$ | $1 \times 10^{-6}$ | – |
| Mechanical quality factor | $Q_m$ | 80 | No data | – |

acoustic source with respect to the real part of the total required electrical input power $P_{in,real}$, and is formulated as follows:

$$\eta_{OE} = \frac{P_{rad}}{P_{in}}, \tag{12}$$

where $P_{rad}$ is obtained from Eq. (11), and $P_{in}$ is directly obtained by measuring the total power that the power supply unit delivers to the circuit. The power dissipation in both amplifier and actuator units is taken into account in the OE criterion. In this study, the combined actuator-amplifier configurations of three actuators and two amplifiers are investigated; the actuation unit includes the two chosen piezoelectric stack devices and a voice coil device, and the amplifier driver unit includes a class AB and a class D amplifier.

To simulate the three complete electrical circuits of the lumped acoustic source, amplifiers, and actuators in time domain, an open access electrical software package called LTspice IV is used [53]. The peak values of the supplied sinusoidal voltage signals are 2 V and 9.75 V, respectively, for voice coil and piezoelectric elements. For the piezoelectric element, a DC offset of 10.8 V is added to the AC signal. For the voice coil actuator, on the other hand, no offset is required in the supplied input signal. For the case where a voice coil device is the actuator, a large resistor ($R_a = 500 \times R_{rad}$) is used in parallel with the element that represents the cavity. The reason is to avoid an unloaded acoustic source at very low frequencies around 20 Hz. In the electrical circuit of a class D amplifier, which is shown in Fig. 5, both diodes and switches are ideal. It is of high importance to model the class D amplifier close to reality. To make a realistic class D amplifier, a parasitic capacitor with the value of $C_{parasitic} = 100$ pF is used between the PWM node and the ground. The on and off resistances of the switches are $R_{on} = 1 \Omega$ and $R_{off} = 1 M\Omega$, respectively. To avoid spikes caused by numerical artifacts during the simulation in LTspice IV, two small auxiliary inductors with a value of $L_{auxiliary} = 4$ nH are connected in series to the two switches. For the realistic class D amplifier, the output signal enters an inductor that is used to recover the reactive power. The values of the inductors are $L = 50$ μH and $L = 146.67$ μH, respectively for voice coil and piezoelectric actuators. A low-pass filter is used in the output port of the class D amplifier to obtain a smooth voltage signal with low ripple. This filter includes a capacitor of $C = 1$ μF. For the piezoelectric device, a resistor of $R = 10 \Omega$ is considered in series with $C$. It has to be noted that all components of the lumped acoustic source in Eqs. (5)–(9) are taken into account in the numerical simulation in LTspice IV. In particular, the frequency dependent terms in Eq. (9) are modeled using LTspice IV in combination with MATLAB R2015b.

### 3.4. Experimental study

The measurements are performed on the thin acoustic source with various actuator-amplifier combinations. The thin acoustic source is schematically shown in Fig. 12 (see Table 4 for details on properties of the source). Voice coil and PZT piezoelectric actuators, with specifications shown in Tables 5 and 6, are used in the measurements. The single crystal PZN-PT piezoelectric actuator modeled in the numerical simulation is not used in the measurements. The reason is that single crystal piezoelectric materials are only available in individual thin layers. Stacking the thin layers to build a long single crystal piezoelectric stack actuator is not straight-forward. Therefore, in the experimental study in this paper, the PZN-PT piezoelectric actuator is not included. Further experimental investigation on the OE of the PZN-PT actuators can be done in future work. PZT piezoelectric device with the optimum length of $l_p = 73.3$ mm does not fit in the air cavity. A motion-converter auxiliary mechanism is used in combination with the piezoelectric actuator in the measurement (see Refs. [54]). The stiffness of the added auxiliary mechanism affects the overall stiffness of the actuation unit and the associated resonance frequencies. The applied voltages to the actuators are the same values used in LTspice IV simulation. Detailed information related to the amplifiers used in the measurements are shown in Fig. 13 and Table 7.

To measure the output radiated power of the thin acoustic source, the central microphone shown in Fig. 14 is used. The microphone manufactured by Microtech Gefell GmbH (model MG M370) [59], is located in the center of the radiating surface and is mounted 17 mm above the surface of the source on a line perpendicular to the surface. The measured near-field sound pressure by the central microphone ($p_{rad}$), the velocity of the vibrating surface ($u$), and the phase difference between them, are used to evaluate the radiated power of the acoustic source. Using the electrical analogy shown in Fig. 10, the volume velocity can be obtained as:
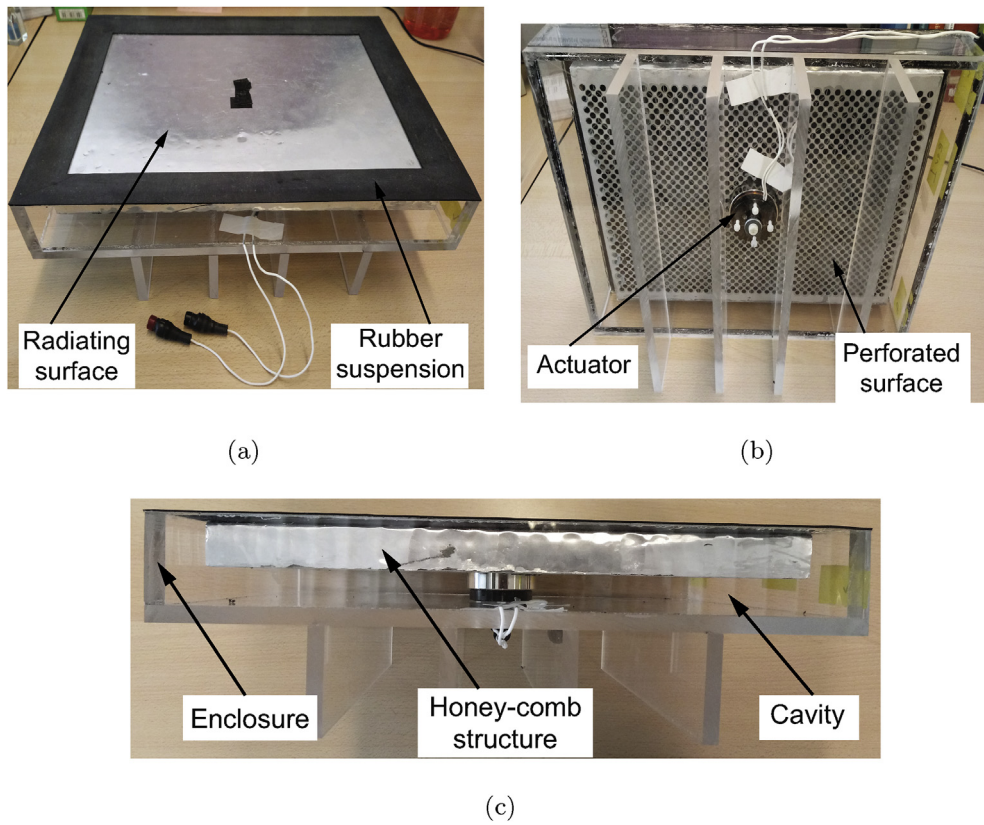
$$U_d = A u, \tag{13}$$

**Fig. 12.** The thin acoustic source that is used in the measurements: (a) top view; (b) bottom view; (c) side view.
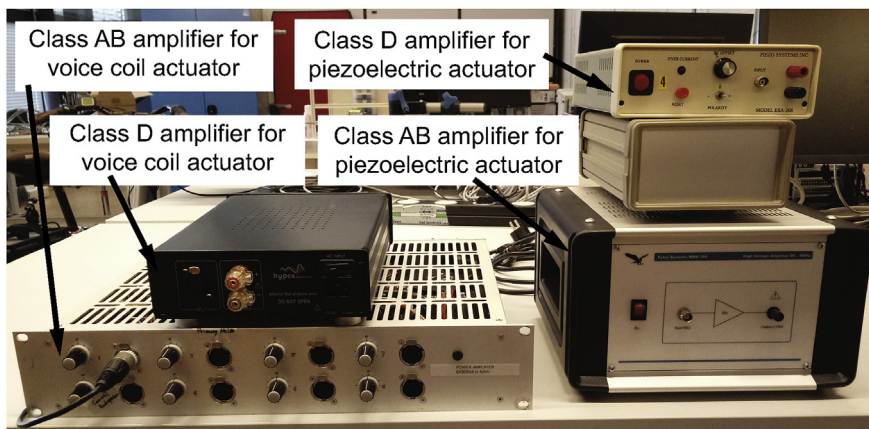


**Fig. 13.** Class AB and class D amplifiers used in the measurements.

and one can evaluate the acoustical radiated power using the following equation:

$$P_{rad} = p_{rad} U_d, \tag{14}$$

where $P_{rad}$ is the measured near-field instantaneous radiated power of the source on a center point mounted 17 mm above the surface of the source.

### 3.5. Results and discussion

The results of numerical simulation in LTspice IV and measurements are shown in Fig. 15(a) and (b), respectively. It has to be noted that the obtained results are shown in the logarithmic scale. This is because in the low frequency range, the CE and

**Table 7**
Properties of the amplifiers used in the measurements.

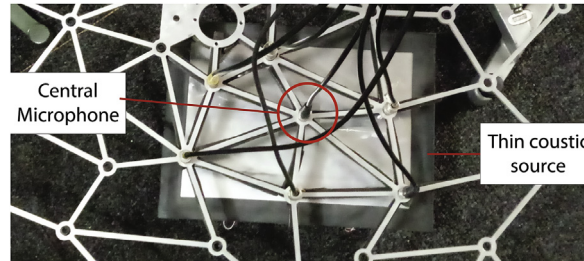| Name | Type | Compatible with | *Pout, max* |
|---|---|---|---|
| Falco Systems WMA-300 [55] | Class AB | PZT | 22.5W |
| Piezo Systems Inc-model ESA-208 [56] | Class D | PZT | 45W |
| ILP Direct LTD model HY2001 [57] | Class AB | Voice coil | 30W |
| Hypex NC400 mono kit [58] | Class D | Voice coil | 200W |



**Fig. 14.** The measured data from the microphone located in the center is used to obtain the radiated power of the thin acoustic source.

OE for the acoustic sources are very low. Therefore, disregarding the definition for the efficiency, the obtained efficiency at low frequencies is not more than $1 \times 10^{-4}$% (see OE in Fig. 15 and CE in Fig. 16). This suggests that a logarithmic scale of the y-axis in both Figs. 15 and 16 gives useful information regarding a better comparison of the combined amplifiers and actuators. The obtained OE from both numerical simulations and measurements show similar behavior in the frequency range of study in this paper.

However, it is not possible to compare the absolute values in these two studies. This is due to the assumption made in the numerical simulation. This assumption is that amplifiers are connected to their maximum load. The analytical efficiencies of the amplifiers are evaluated for the case in which the amplifiers are operating at their maximum power. In the measurements, on the other hand, it was not possible to apply maximum loads to the amplifiers. Therefore, the obtained values from the numerical simulations may not be compared to those from the measurements. But the behavior in the two studies can be compared. The fluctuations seen in Fig. 15(a) are due to averaging the obtained results from time domain analysis in LTspice IV. Therefore, these fluctuations do not have physical meanings.

As seen in both numerical and experimental results, an acoustic source connected to a piezoelectric actuator has a fundamental resonance at higher frequencies compared to that for an acoustic source that is connected to a voice coil actuator. The numerical simulation in Fig. 15(a) predicts the first resonance frequency of the acoustic source that is connected to piezoelectric actuators to be above 1000 Hz, which is not within frequency range of interest in this paper (between 20 Hz and 1000 Hz). The measurement, on the other hand, shows that the first resonance frequency of the same acoustic source actuated by a PZT piezoelectric device occurs at approximately 370 Hz (see Fig. 15(b)). This difference between the numerical and the experimental results is due to the usage of the auxiliary mechanism that is connected to the PZT in the measurement. The connected auxiliary mechanism changes the overall stiffness of the actuator and results in a different resonance frequency of the acoustic source [54]. According to Fig. 15, in both numerical and experimental studies, the first resonance frequency of the voice coil actuator occurs approximately at 170 Hz, that is within the frequency range of study. Fig. 15 shows that in both numerical and experimental studies, at higher frequencies (above 800 Hz) and without considering the effect of connected amplifiers, using the two piezoelectric actuators leads to a higher OE of the acoustic source than using a voice coil actuator. However, below 800 Hz, piezoelectric actuators that are connected to a class AB amplifier have the lowest OE. The reason is that in this frequency range, the majority of the input power is stored in the piezoelectric actuators, while no energy recovery is possible in a class AB amplifier.

According to Fig. 15(a) and (b), the acoustic source actuated by a voice coil device has its fundamental resonance at 170 Hz. This resonance corresponds to the maximum OE of the acoustic source that is actuated by a voice coil device in the frequency range of study. At frequencies near 170 Hz, the OE of the acoustic source actuated by a voice coil actuator is affected by this resonance. Fig. 15 shows that when a class D amplifier is the driver, except for a small range of frequencies near resonance of the voice coil, the OE of a PZT device is higher than a voice coil element. The location of the resonance mainly depends on the size and geometry of the voice coil element. For the voice coil actuator that is used in this study, the mass is the reference for a fair comparison. This voice coil actuator results in a resonance near 170 Hz. However, by choosing the voice coil actuator and its mechanical damping appropriately, the sharp resonance in this frequency range can be damped.

The numerical study shows that the combination of a PZN-PT piezoelectric actuator and a class D amplifier results in the highest OE of the acoustic source over the entire frequency range of study (see Fig. 15(a)). According to both numerical and experimental studies (see Fig. 15(a) and (b)), for the case of a PZT piezoelectric device that is connected to a class D amplifier, a higher OE than a voice coil device is seen almost in the entire frequency range of study. As it is mentioned earlier, near the resonance frequency of the acoustic source that is actuated by the voice coil actuator, the OE of the voice coil source is slightly higher. Both numerical and measurement results show that the higher efficiency of the piezoelectric elements, particularly
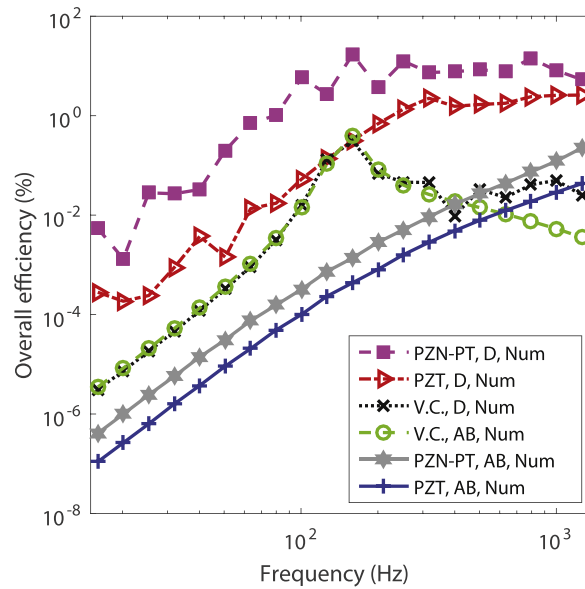
(a)
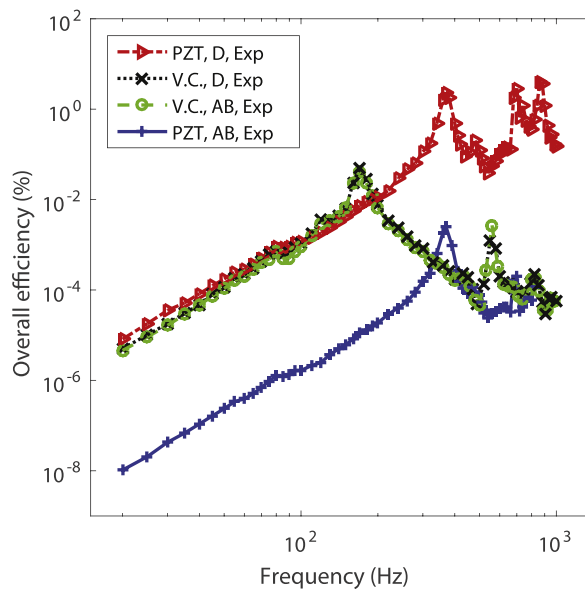


(b)

**Fig. 15.** The overall efficiency of the thin acoustic source that is connected to various combined configurations of amplifier-actuator: (a) numerical; (b) experimental.

at frequencies below 100 Hz, is due to recovering the reactive power stored in the acoustic source using a class D amplifier. This energy recovery leads to an increase in the OE of the acoustic source. As it was mentioned earlier, even when a voice coil actuator, which is off the resonance, is driven by a class D amplifier, not so much power can be recovered. The reason is that in this case, high power dissipation occurs twice in the voice coil element; both during charge and recovery cycles. Consequently, not so much power can be recovered and reused eventually, especially in the low frequency range below 100 Hz.

As seen in both numerical and experimental results (Fig. 15), when a voice coil device is the actuator, the two classes AB and D amplifiers have similar influence on the performance of the acoustic source. The reason is that in this case, prior to the immediate power dissipation peak in the actuator unit during the charge cycle, a part of the power is dissipated in the amplifier unit. In a class AB amplifier, power dissipation occurs due to the continuous voltage drop across the transistors during the charge cycle. In a class D amplifier, on the other hand, power dissipation related to switching cycles is negligible during charge.
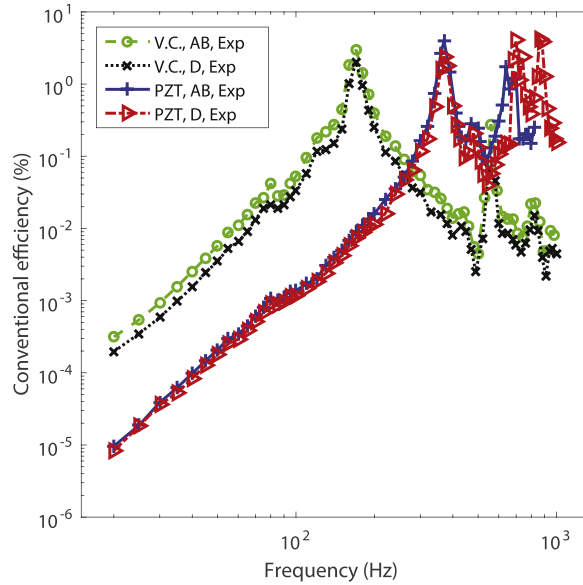
**Fig. 16.** The conventional efficiency of the thin acoustic source that is connected to various combined configurations of amplifier-actuator. The graph is derived from experiment.

Depending on the connected amplifier, the power dissipation in the discharge cycle occurs either immediately in a class AB amplifier or in the case of a class D amplifier, again in the actuator unit during the energy recovery cycle. Therefore, the overall power dissipation in both amplifiers is relatively similar. This leads to a relatively similar OE for the two amplifiers.

According to Fig. 15, both numerical and experimental studies predict that an acoustic source actuated by a voice coil device can hardly reach the OE of 0.4% over the entire frequency range of interest. In fact, the highest OE for the voice coil actuator occurs at the resonance frequency (170 Hz). On the other hand, the numerical simulation shows that the configuration of a single crystal piezoelectric device connected to a class D power driver reaches the highest OE with a maximum of 18% over the entire frequency range (see Fig. 15(a)). According to both numerical and experimental studies in Fig. 15, a PZT piezoelectric actuator connected to a class D amplifier can achieve higher OEs of the acoustic source with a maximum of 8% compared to a voice coil device.

The CE, on the other hand, neglects the power flow in the amplifier unit. According to the experimental result in Fig. 16, the CE of the acoustic source is independent of the amplifiers' type. According to the measurement result, the acoustic source that is actuated by a voice coil device has a higher CE than the source that is actuated by a PZT piezoelectric device.

When the voice coil device is the actuator, a comparison between the experimental results in Figs. 15(b) and 16 shows that at the low frequency of 20 Hz, CE = $2 \times 10^{-4}$% and OE = $5 \times 10^{-6}$%. Using Eq. (3), the efficiency of the connected amplifiers can be determined to be 2.5% for both amplifier cases. The reason is that for the class AB amplifier, the output voltage has an amplitude of $V_{actuator} = 2$ V, whereas the supply voltage to the amplifier is $V_{supply} = \pm30$ V (see Fig. 4 and Ref. [57]). The theoretical efficiency of the amplifier can be obtained as $\frac{\pi}{4}V_{actuator}/V_{supply}$ for the maximum output voltage. For a class AB amplifier with the output voltage of 2 V, the theoretical efficiency is as low as 5.2%, disregarding the quiescent current. If the quiescent current is taken into account, the amplifier efficiency can drop to 2.5%. This is in accordance with the measured amplifier efficiency of 2.5%. For the class D amplifier, the output voltage amplitude and the supply voltage are respectively $V_{actuator} = 2$ V and $V_{supply} = \pm50$ V (see Fig. 5 and Ref. [58]). These lead to the amplifier efficiency of approximately 6%. This amplifier efficiency is almost in the same order of magnitude as the efficiency obtained from the measurement and is aligned with the calculated efficiency from Figs. 15(b) and 16.

Fig. 16 shows the importance of taking the amplifier unit into account in order to have a fair comparison between the actuation units of the acoustic source. The experimental results in Figs. 15(b) and 16 show that an OE is a more reliable criterion than a CE to define the performance of an acoustic source.

## 4. Conclusion

In the present research, a criterion called overall efficiency (OE) is defined that is in particular interesting in application of acoustic sources at low frequencies (from 20 Hz to 1000 Hz). Since the OE criterion takes the effect of connected amplifiers and actuators units into account, it gives an overview about the power loss and power storage in the loudspeaker systems. Experimental results reveal that the OE is a more reliable criterion to compare the performance of acoustic sources. In a case study, a flat acoustic source, which is the same size as a standard $A_4$ paper (297 mm × 210 mm) is numerically and experimentally stud-

ied. The flat source is connected to various actuator-amplifier configurations, and in particular is examined in a low frequency range between 200 Hz and 1000 Hz. The dependency of the OE on the operating frequency, the phase difference between the current and voltage and the reactive nature of the connected actuator is investigated using the flat acoustic source. Piezoelectric and voice coil actuators are compared. It is numerically shown that a single crystal piezoelectric element driven by a class D amplifier results in the highest OE for the acoustic source in the entire frequency range of study. Moreover, both numerical and experimental studies show that a PZT piezoelectric device connected to a class D amplifier can lead to higher OEs than an off-the-resonance voice coil actuator, especially at frequencies below 100 Hz. Among the actuator-amplifier configurations that are taken into account in the numerical study, a single crystal piezoelectric actuator reaches the highest OE of 18%, while the PZT actuator can lead to an OE of 8%. On the other hand, the lowest OE of the acoustic source is obtained when piezoelectric actuators are connected to a class AB amplifier. This low OE is due to the capacitive nature of the piezoelectric element at low frequencies. Therefore, the large amount of reactive power stored in the piezoelectric devices cannot be recovered when a class AB amplifier is used. In addition, it is shown that for a voice coil actuator, it does not really matter which amplifier is the driver. A similar OE for the acoustic source is obtained using both amplifiers. The numerical simulation results are in a good agreement with those obtained from the measurements to successfully predict the behavior of combined amplifier-actuator-acoustic source systems.

## Credit author statement

Farnaz Tajdari: Conceptualization, Methodology, Software, Validation, Formal analysis, Investigation, Writing - original draft. Arthur P. Berkhoff: Supervision, Writing- Reviewing and Editing. Ronan R.A.R van der Zee: Writing- Reviewing and Editing, Supervision. André de Boer: Writing- Reviewing and Editing, Supervision.

## Declaration of competing interest

The authors declare that they have no known competing financial interests or personal relationships that could have appeared to influence the work reported in this paper.

## Acknowledgements

## References

[1] S.J. Elliott, P.A. Nelson, Active noise control, IEEE Signal Process. Mag. 10 (4) (1993) 12–35, https://doi.org/10.1109/79.248551.
[2] W.P.J. de Bruijn, M.M. Boone, Application of wave field synthesis in life-size videoconferencing, in: Audio Engineering Society Convention, vol. 114, 2003, http://www.aes.org/e-lib/browse.cfm?elib12606.
[3] R. Small, Direct-radiator loudspeaker system analysis, IEEE Trans. Audio Electroacoust. 19 (4) (1971) 269–281, https://doi.org/10.1109/TAU.1971.1162200.
[4] N.J. Harris, IEE Proc. Circ. Dev. Syst. 147 (4) (2000) 153–157, https://doi.org/10.1049/ip-cds:20000390.
[5] N. Harris, M.J. Hawksford, The distributed-mode loudspeaker (dml) as a broad-band acoustic radiator, in: Audio Engineering Society Convention, vol. 103, 1997, http://www.aes.org/e-lib/browse.cfm?elib7253.
[6] J. Panzer, N. Harris, Distributed-mode loudspeaker radiation simulation, in: Audio Engineering Society Convention, vol. 105, 1998, http://www.aes.org/e-lib/browse.cfm?elib8397.
[7] O. Pabst, J. Perelaer, E. Beckert, U. Schubert, R. Eberhardt, A. Tnnermann, Inkjet Printing of Electroactive Polymer Actuators on Polymer Substrates, 2011https://doi.org/10.1117/12.878873.
[8] O. Pabst, E. Beckert, J. Perelaer, U.S. Schubert, R. Eberhardt, A. Tnnermann, All Inkjet-Printed Electroactive Polymer Actuators for Microfluidic Lab-On-Chip Systems, 2013https://doi.org/10.1117/12.2009605.
[9] Z. Zhao, C. Shuai, Y. Gao, E. Rustighi, Y. Xuan, An application review of dielectric electroactive polymer actuators in acoustics and vibration control, J. Phys. Conf. 744 (1) (2016) 12162. http://stacks.iop.org/1742-6596/744/i1/a012162.
[10] O. Heuss, W. Kaal, T. Klaus, C. Thyes, J. Tschesche, R. Karsten, Design approach for an active double-glazed window, in: Proceedings of the International Conference on Noise and Vibration Engineering ISMA 2014, Leuven, Belgium, 2014, pp. 77–91. http://past.isma-isaac.be/downloads/isma2014/papers/isma2014_0365.pdf.
[11] H. Wen-chao, N. Chung-fai, Sound insulation improvement using honeycomb sandwich panels, Appl. Acoust. 53 (13) (1998) 163–177, https://doi.org/10.1016/S0003-682X(97)00033-9.
[12] C. Ng, C. Hui, Low frequency sound insulation using stiffness control with honeycomb panels, Appl. Acoust. 69 (4) (2008) 293–301, https://doi.org/10.1016/j.apacoust.2006.12.001.
[13] A. Putra, D. Thompson, Sound radiation from perforated plates, J. Sound Vib. 329 (20) (2010) 4227–4250, https://doi.org/10.1016/j.jsv.2010.04.020.
[14] M. Vivolo, B. Pluymers, D. Vandepitte, W. Desmet, An experimental-numerical study on the vibro-acoustic characterization of honeycomb lightweight panels, in: Proceedings of the International Conference on Noise and Vibration Engineering ISMA 2010, Leuven, Belgium, 2010, pp. 2197–2211. http://past.isma-isaac.be/downloads/isma2010/papers/isma2010_0486.pdf.
[15] A. Putra, D. Thompson, Radiation efficiency of unbaffled and perforated plates near a rigid reflecting surface, J. Sound Vib. 330 (22) (2011) 5443–5459, https://doi.org/10.1016/j.jsv.2011.05.033.
[16] M. Toyoda, D. Takahashi, Reduction of acoustic radiation by impedance control with a perforated absorber system, J. Sound Vib. 286 (3) (2005) 601–615, https://doi.org/10.1016/j.jsv.2004.10.011.
[17] M. Toyoda, M. Tanaka, D. Takahashi, Reduction of acoustic radiation by perforated board and honeycomb layer systems, Appl. Acoust. 68 (1) (2007) 71–85, https://doi.org/10.1016/j.apacoust.2005.11.011.
[18] O. Cherrier, V. Pommier-Budinger, F. Simon, Panel of resonators with variable resonance frequency for noise control, Appl. Acoust. 73 (8) (2012) 781–790, https://doi.org/10.1016/j.apacoust.2012.02.011.
[19] M. Regniez, F. Gautier, C. Pezerat, A. Pelat, Acoustic impedance of microperforated honeycomb panels, in: Proceedings of 1st Euro-Mediterranean Conference on Structural Dynamics and Vibroacoustics, 2013, pp. 364–367. https://medyna2013.sciencesconf.org/conference/medyna2013/Medyna2013_proceedings.pdf.

[20] B. Petitjean, I. Legrain, F. Simon, S. Pauzin, Active control experiments for acoustic radiation reduction of a sandwich panel: feedback and feedforward investigations, J. Sound Vib. 252 (1) (2002) 19–36, https://doi.org/10.1006/jsvi.2001.4022.
[21] A. Berkhoff, Sound generator, US Patent, US20 vol. 100 111 351 A2 (2010). URL https://nl.espacenet.com/publicationDetails/originalDocument?DBEPODOClocalenl_nlFTD&date20100506CCUSNR2010111351A1KCA1#.
[22] J. Ho, A. Berkhoff, Flat acoustic sources with frequency response correction based on feedback and feed-forward distributed control, J. Acoust. Soc. Am. 137 (4) (2015) 2080–2088, https://doi.org/10.1121/1.4914997.
[23] J. Ho, Control Source Development for Reduction of Noise Transmitted through a Double Panel Structure, Ph.D. thesis, University of Twente, Enschede, The Netherlands, Jully 2014https://doi.org/10.3990/1.9789036537025.
[24] C. Wallenhauer, A. Kappel, B. Gottlieb, T. Schwebel, T. Lth, Efficient class-b analog amplifier for a piezoelectric actuator drive, Mechatronics 19 (1) (2009) 56–64, https://doi.org/10.1016/j.mechatronics.2008.06.009.
[25] C. Wallenhauer, B. Gottlieb, R. Zeichfl, A. Kappel, Efficiency-improved high-voltage analog power amplifier for driving piezoelectric actuators, IEEE Trans. Circ. Syst. I: Regul. Pap. 57 (1) (2010) 291–298, https://doi.org/10.1109/TCSI.2009.2018938.
[26] T. Horn, J. Melbert, A linear 10 kv power amplifier for piezo actuators, in: Proceedings of 6th International Conference on Integrated Power Electronics Systems, 2010, pp. 1–5. https://ieeexplore.ieee.org/stamp/stamp.jsp?arnumber57 30655.
[27] M. Chiaberge, A. Tonoli, G. Botto, M. De Giuseppe, S. Carabelli, F. Maddaleno, Model and design of a power driver for piezoelectric stack actuators, EURASIP J. Embed. Syst. 2010 (1) (2010) 578–591, https://doi.org/10.1155/2010/578591.
[28] D. Campolo, M. Sitti, R. Fearing, Efficient charge recovery method for driving piezoelectric actuators with quasi-square waves, IEEE Trans. Ultrason. Ferroelectrics Freq. Contr. 50 (3) (2003) 237–244, https://doi.org/10.1109/TUFFC.2003.1193617.
[29] C.-S. Chao, P.-C. Huang, M.-K. Chen, L.-S. Jang, Design and analysis of charge-recovery driving circuits for portable peristaltic micropumps with piezoelectric actuators, Sensor Actuator Phys. 168 (2) (2011) 313–319, https://doi.org/10.1016/j.sna.2011.04.027.
[30] H. Liang, Z. Jiao, R. Zhang, X. Wang, X. Liu, Design of a power amplfier with energy recovery strategy for piezoelectric actuators, in: Proceedings of 2011 International Conference on Fluid Power and Mechatronics, 2011, pp. 207–212, https://doi.org/10.1109/FPM.2011.6045758.
[31] D. Vasic, F. Costa, Energy recovery power supply for piezoelectric actuator, in: IECON 2014 - 40th Annual Conference of the IEEE Industrial Electronics Society, 2014, pp. 1440–1445, https://doi.org/10.1109/IECON.2014.7048691.
[32] D. Wang, W. Zhu, Q. Yang, W. Ding, A high-voltage and high-power amplifier for driving piezoelectric stack actuators, J. Intell. Mater. Syst. Struct. 20 (16) (2009) 1987–2001, https://doi.org/10.1177/1045389X09345559.
[33] G. Gnad, R. Kasper, A power drive control for piezoelectric actuators, in: 2004 IEEE International Symposium on Industrial Electronics, vol. 2, 2004, pp. 963–967, https://doi.org/10.1109/ISIE.2004.1571944.
[34] W.P. Robbins, Simplified unipolar, quasisquare wave energy recovery drive circuits for piezoelectric actuators, IEEE Trans. Ultrason. Ferroelectrics Freq. Contr. 52 (8) (2005) 1420–1426, https://doi.org/10.1109/TUFFC.2005.1509802.
[35] B. Edamana, K. Oldham, Optimal low-power piezoelectric actuator control with charge recovery for a microrobotic leg, IEEE ASME Trans. Mechatron. 18 (1) (2013) 251–262, https://doi.org/10.1109/TMECH.2011.2165079.
[36] H. Janocha, C. Stiebel, New approach to a switching amplifier for piezoelectric actuators, in: Proc. 6th Internat. Conference on New Actuators, 1998, pp. 189–192. http://www.lpa.uni-saarland.de/pdf/Actuator98.pdf.
[37] C. Stiebel, H. Janocha, New Concept of a Hybrid Amplifier for Driving Piezoelectric Actuators, vol. 33, 2000, pp. 365–370, https://doi.org/10.1016/S1474-6670(17)39171-1. 26.
[38] H. Janocha, C. Stiebel, T. Wrtz, Power Amplifiers for Piezoelectric Actuators, Springer Netherlands, Dordrecht, 2002, pp. 379–391, https://doi.org/10.1007/978-94-010-0483-1_14.
[39] A. Ballato, Modeling piezoelectric and piezomagnetic devices and structures via equivalent networks, IEEE Trans. Ultrason. Ferroelectrics Freq. Contr. 48 (5) (2001) 1189–1240, https://doi.org/10.1109/58.949732.
[40] Q. Gallas, R. Holman, T. Nishida, B. Carroll, M. Sheplak, L. Cattafesta, Lumped element modeling of piezoelectric-driven synthetic jet actuators, AIAA J. 41 (2) (2003) 240–247, https://doi.org/10.2514/2.1936.
[41] S. Horowitz, M. Sheplak, L. Cattafesta III, T. Nishida, A mems acoustic energy harvester, J. Micromech. Microeng. 16 (9) (2006) S174–S181, https://doi.org/10.1088/0960-1317/16/9/S02.
[42] S. Prasad, Q. Gallas, S. Horowitz, B. Sankar, L. Cattafesta, M. Sheplak, Analytical electroacoustic model of a piezoelectric composite circular plate, AIAA J. 44 (10) (2006) 2311–2318, https://doi.org/10.2514/1.19855.
[43] M. Pillai, E. Deenadayalan, A review of acoustic energy harvesting, Int. J. Precis. Eng. Manuf. 15 (5) (2014) 949–965, https://doi.org/10.1007/s12541-014-0422-x.
[44] The great power vs. Energy confusion. https://cleantechnica.com/2015/02/02/power-vs-energy-explanation/, (Accessed 28 April 2020).
[45] F. Tajdari, A. Berkhoff, A. de Boer, Numerical modeling of electrical-mechanical-acoustical behavior of a lumped acoustic source driven by a piezoelectric stack actuator, in: Proceedings of the International Conference on Noise and Vibration Engineering ISMA 2016, KULeuven, Leuven, Belgium, 2016, pp. 1261–1275. http://doc.utwente.nl/102767/.
[46] A. Pierce, Acoustics: an Introduction to its Physical Principles and Applications, Acoustical Society of America, New York, 1989https://doi.org/10.1063/1.2914388.
[47] R.W. Leonard, Generation and Measurement of Sound in Gases, Springer Berlin, Heidelberg, 1962, pp. 1–2, https://doi.org/10.1007/978-3-642-45976-4.
[48] L. Beranek, T. Mello, Acoustics: Sound Fields and Transducers, Academic Press, 2012https://doi.org/10.1016/C2011-0-05897-0.
[49] Specifications,LA18-12-000A, BEI Kimco Magnetics. http://cdn1.beikimco.com/Products/Downloads_vca_frameless/voice-coil-ac tuator-linear-frameless-la18-12-000a.pdf, (Accessed 16 May 2019).
[50] MATLAB optimization toolbox, documentation. https://www.mathworks.com/help/optim/, (Accessed 25 May 2019).
[51] R. Shukla, K.K. Rajan, M. Shanthi, J. Jin, L.-C. Lim, P. Gandhi, Deduced property matrices of domain-engineered relaxor single crystals of [110] L [001] T cut: effects of domain wall contributions and domain-domain interactions, J. Appl. Phys. 107 (1) (2010), https://doi.org/10.1063/1.327042601410210141025.
[52] Specifications, NAC2013-HXX, noliac. http://www.noliac.com/products/actuators/plate-stacks/show/nac2013-hxx/, (Accessed 16 May 2019).
[53] Analog devices, LTspice. https://www.analog.com/en/design-center/design-tools-and-calculators/ltspice-simulator.html, (Accessed 15 May 2019).
[54] F. Tajdari, A. Berkhoff, A. de Boer, Numerical modeling of a flexural displacement-converter mechanism to excite a flat acoustic source driven by piezoelectric stack actuators, in: Proceedings of the International Conference on Noise and Vibration Engineering ISMA 2018, KULeuven, Leuven, Belgium, 2018, https://research.utwente.nl/en/publications/numerical-m odeling-of-a-flexural-displacement-converter-mechanism.
[55] Falco Systems, WMA-300 High speed high voltage amplifier. http://www.falco-systems.com/High_voltage_amplifier_WMA-300.html, (Accessed 16 May 2019).
[56] Piezo systems inc., ESA-208 piezo switching amplifier. http://pdf.dzsc.com/2008722/200807220952515145.pdf, (Accessed 16 May 2019).
[57] ILP direct LTD, HY2001. https://www.digchip.com/datasheets/download_datasheet.php?id3426852part-numberHY2001, (Accessed 24 June 2019).
[58] Hypex, NC400 mono kit,. https://www.diyclassd.com/product/nc400/11, (Accessed 16 May 2019).
[59] Microtech Gefell GmbH, MG M370. https://www.instrumentation.it/gallery/5601/id_M_370_eng.pdf, (Accessed 7 July 2019).